Final Report:
Quantifying advective and nonstationary effects on eddy fluxes in the AmeriFlux network

Project ID 0013717
Prog Mgr Michael Kuperberg Phone: 301-903-3511
Division: SC-23.3
PI: David R. Fitzjarrald
Co-I: Ricardo K. Sakai
Award Register#: ER64359

1. Introduction

Our goal was to study the flows within and above of a forested area and assess the degree to which horizontal subcanopy motions transport significant amounts of CO_2. This process can explain why ecosystem respiration appears to be underestimated on calm nights. It is essential to understand the physical and biological mechanisms that determine relevant processes that occur on these 'suspect' nights. Understanding drainage flows and intermittent mixing at night is only now getting attention in the meteorological community [*Mahrt*, 2008; *Mahrt et al.*, 2001; *Sun et al.*, 2007, 1998]. It is insufficient only to 'gap fill' data [*Falge et al.*, 2001; *Goulden et al.*, 1996], though these are useful interim approaches to assist in making annual budgets.

Our objectives evolved after the first field season to include studies to measure how of flow over Prospect Hill at Harvard Forest affects subcanopy motions. Bernoulli effects associated with flow over hills strongly affect subcanopy motions in wind tunnel and computer simulations, possibly altering horizontal CO_2 advection there [*Belcher and Reading*, 2008; *Finnigan and Belcher*, 2004; *Katul et al.*, 2006; *Poggi and Katul*, 2007; *Ross*, 2008]. These arguments, based on scale analyses, wind tunnel experiments, and large eddy simulations, have not been confirmed by observations. *Thomas and Foken* [2007] examined turbulent mixing scales at one site, but they concentrated on convective, neutral and weakly stable conditions, with nearly continuous turbulent mixing. In our earlier work, we saw no evidence for such effects [*Staebler and Fitzjarrald*, 2004]. We believe that a major uncertainty is how one characterizes turbulent mixing under the strongly stable, weak wind conditions that obtain in the subcanopy when drainage flows occur and the supposed pressure gradient perturbations that would drive 'counterflows' might both be present. Models simulate vertical mixing inside the

canopy by specifying mixing lengths (or equivalents), empirical guides whose empirical origin is based on observations made of continuously mixing flows. Wind tunnel studies suffer from difficulties to realize the complex pattern of vertical stability in canopies. Our results indicate that the forest floor is more strongly decoupled from the flow aloft than has been modeled.

To test the 'flow over hill' hypothesis, we set out during the 2009 field observation campaign to complement our ongoing work with sensors designed to obtain observations to document the flow over topography at Harvard Forest. We continued to operate the subcanopy array at the Little Prospect Hill (LPH) tract. In 2009 season, we installed two sodars (acoustic radars; details below). *Karipot et al.* [2006] and *Leclerc et al.* [2003], among others, showed that sodar observations are useful to help understand advective processes near flux towers, but they did not explicitly examine influences of flows over nearby hills. *In 2011, after the formal period of this project ended, we used other funds to operate a sodar at the Hemlock Tower field site* (see Fig. 1). In this way we could categorize above-canopy flows by direction and intensity, compare flow upwind and downwind of the major topographic features, and determine the extent to which subcanopy flows are altered. The final step is to document if any effects are sufficient to modify the role of horizontal advection on the subcanopy CO_2 budget.

Though we had insufficient instrumentation to field subcanopy arrays at the LPH and EMS sites simultaneously, we fill this void using data archived during the 1998-2003 studies [*Staebler and Fitzjarrald*, 2004]. We formed composites of subcanopy motion stratified by wind speed and direction just above the canopy. For a selected period in 2002, we operated two sodars, one well upwind of Prospect Hill and one adjacent to the EMS tower. The task has outlived the funding source; we will pursue this topic until we complete it.

2. Sites and instrumentation

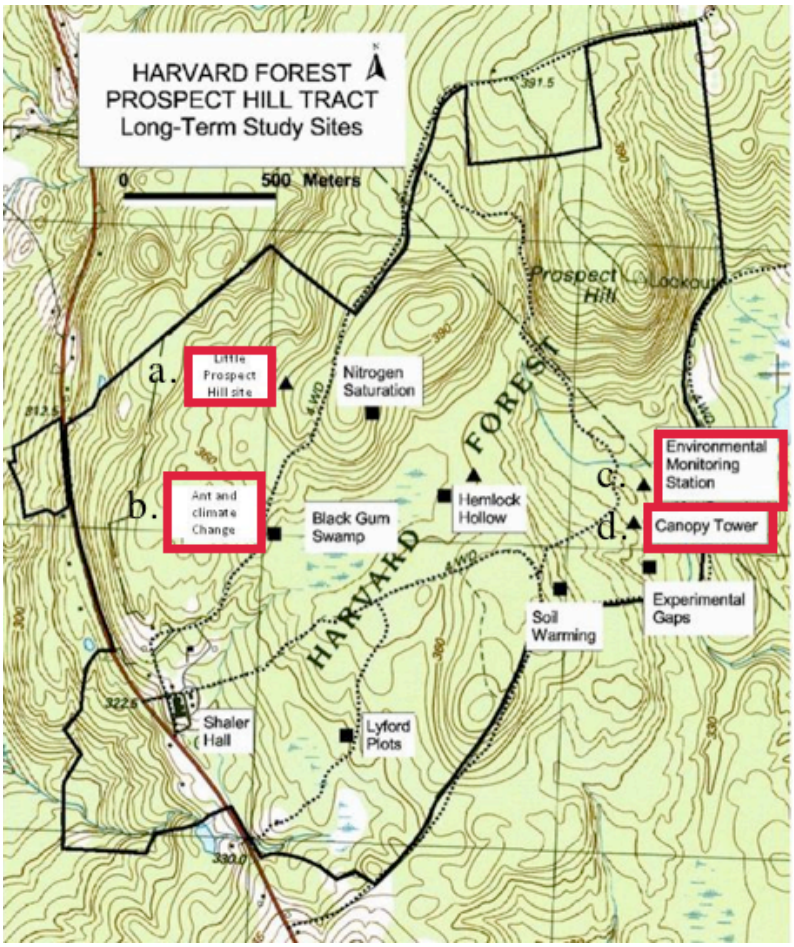

Figure 1. Current research sites at Harvard Forest. Red borders locate a) Little Prospect Hill tract (flux tower and subcanopy array), b) the Ant and Climate Change plot (sodar PA0), c) the Environmental monitoring site (flux tower) d) the EMS canopy tower (PA0 sodar) and e) the Hemlock tower site. (map adapted from the Harvard forest web site.)

Harvard Forest (Petersham, MA; 42°30'30" N; 72°12'28" W) is a transition mixed deciduous and conifer forest. The dominant species are rRed oak (*Quercus rubra*), red maple (*Acer rubrum*), black birch (*Betula lenta*), white pine (*Pinus strobus*), and eastern hemlock (*Tsuga canadensis*). There are three flux towers, the Environmental Monitoring Station (EMS), at the Hemlock Hollow site (HS), and at the Little Prospect Hill site (LPH) (fig. 1). At EMS, we did earlier work investigating the role of subcanopy motions on CO_2 budgets [*Staebler and Fitzjarrald*, 2004, 2005]. In 2011 we operated a sodar at the Hemlock tower site.

Figure 2. May 2009 Remtech PA1 sodar installation at the Ant and Climate Change experiment.

The LPH site, where a subcanopy array of sonic anemometers where installed around the flux tower at 1.7 m. Locations and instrument types are described in Tables 1 and 2 for the subcanopy array and tower flux deployments respectively. Also to complement the existent set up at LPH, the tower flux has been equipped to have a more refined wind, temperature, and humidity profile (table 2). The tower flux measures continuously throughout the year. The subcanopy array set up measurement campaign is shown in Table 3. Airflow measurements using sodars has been done in 2000, 2002, 2008, and 2009. In 2009, two sodars were installed at the EMS site (Remtech, model PA0) and at the Ant and Climate Change experiment (Remtech, model PA1) to monitor the flow over the terrain (fig. 1).

A flexible data acquisition system based on the open-source Linux operating system has been used for several years. The data are sent to the computers as serial streams where they are collected and synchronized by computer software. It calculates the statistical moments until the 4th order, cross correlations, and spectral analysis. The desktop can collect up to 32 serial lines using serial port expansion boards. For the analog signals, such as temperature and relative humidity probes, Campbell dataloggers are used to convert to serial signals. The subcanopy array system corresponds to a four-point subcanopy wind speed (AIR, model SPAS 2Y) and CO_2 concentration around the flux tower. One closed path CO_2/H_20 sensor (Licor, LI7000) controlled by a Valco solenoid valve is measuring all the horizontal CO_2 concentrations (Table 1).

Table 1: Subcanopy array the sonic anemometers and CO_2 sampling during the 2008/2009 field observations. (Coordinate origin is LPH flux tower).

ID	ID, parameters	x(m)	y(m)	z(m)	Instrument
2D1	*u, v, Ts,* H_2O, CO_2	-5.9	43.8	-5.4	ATI 2D sonic, model SPASS/2Y; licor, model LI700
2D2	*u, v, Ts,* H_2O, CO_2	-63.2	-18.2	0.4	ATI 2D sonic, model SPASS/2Y; licor, model LI700
2D3	*u, v, Ts,* H_2O, CO_2	-28.9	77.2	7.5	ATI 2D sonic, model SPASS/2Y; licor, model LI700
2D4	*u, v, Ts,* H_2O, CO_2	75.3	18.1	3.0	ATI 2D sonic, model SPASS/2Y; licor, model LI700
Gill3D	*u, v, w, Ts,* H_2O, CO_2	2.4	-12.8	2.0	Gill Research 3D sonic; licor, model LI700

Table 2: LPH flux tower observations.

Parameters	z(m)	Instrument
Q*	27.0	Kipp & Zonen, model NR-LITE (*)
PARdw	21.0	Licor, model 190SB (*)
u,v,w,Ts, CO_2, H_2O	21.0	Campbell Sci. sonic anemometer, model CSAT/ Licor gas analyzer, model 7000 (10 Hz sampling rate) (*)
T, RH, CO_2	21.0	Vaisala, model HMP45C/ Licor, model LI820 (*)
CO_2	16.0	Licor, model LI820 (*)
CO_2	10.0	Licor, model LI820 (*)
T,RH	9.2	Vaisala HMP45C
u,v,w,Ts	7.2	ATI 3D sonic anemometer, K model
CO_2	5.0	Licor, model LI820 (*)
u, v, Ts	3.9	ATI 2D sonic sonic SPASS/2Y
T,RH	3.5	Vaisala HMP 45C
CO_2	2.0	Licor, model LI820 (*)
T,RH	1.6	Vaisala 50Y
CO_2	1.0	Licor, model LI820 (*)
T,RH	0.5	Vaisala 50Y
CO_2	0.3	Licor, model LI820 (*)
CO_2	0.1	Licor, model LI820 (*)

(*) LPH tower original set up (Julian Hadley, personal communication).

3. Results

Despite suffering lightning damage at the LPH in July of 2007, 2008, 2009, and in 2011, we have archived much data (Table 3).

Table 3: Periods with subcanopy array measurements.

Period, Year	Dates
Summer 2008 (Spr08)	29/06/2008 – 07/29/2008
Fall 2008 (Fall08)	09/18/2008 – 30/10/2008
Winter 2008/2009 (Win09) *	30/10/2008 – 04/15/2009
Spring 2009 (Spr09)	04/15/2009 – 06/08/2009

** Subcanopy CO_2 measurements paused on 01/14/2009 and resumed on 4/15/2009.*

a. Subcanopy airflow at the LPH site.

A remarkable feature of the wind flow within the canopy at LPH is a diurnal motion pattern largely decoupled from the wind aloft (Figs. 3 and 4). The subcanopy flow is very organized, with the spatial wind steadiness (the ratio between the mean vector modulus and the mean scalar wind) generally > 0.9. Subcanopy flow follows the local topographic gradient: At night the flow is katabatic (downslope) and during the day it is anabatic (upslope). This strongly suggests that a thermal driven process drives the understory winds, even during daytime. This pattern persists even when the canopy was leafless (Fig. 4). Temperature gradients from tower measurements indicate that at night the atmosphere is stable in the lowest part of the understory environment but slightly convective in the top of understory. During the day, the entire subcanopy layer was slightly convective. Seasonal differences in the subcanopy flow are related to the intensity of the uphill/downhill winds. During the summer, there are stronger downhill winds, whereas during winter the uphill and winds with the above-canopy direction prevail. The winds at the top of the tower have a strong westerly component that is the synoptic pattern in this region. In summer, it is predominantly SW. During fall and winter, winds are more westerly and northwesterly, and in the spring W. However, a more detailed look at the 21 m winds (tower top) indicates that there are topographic effects evident in the hodographs even the canopy is fully leafed. If the above-canopy mean wind is subtracted from the hodographs, there is an oscillation similar to that observed at the subcanopy levels in summer.

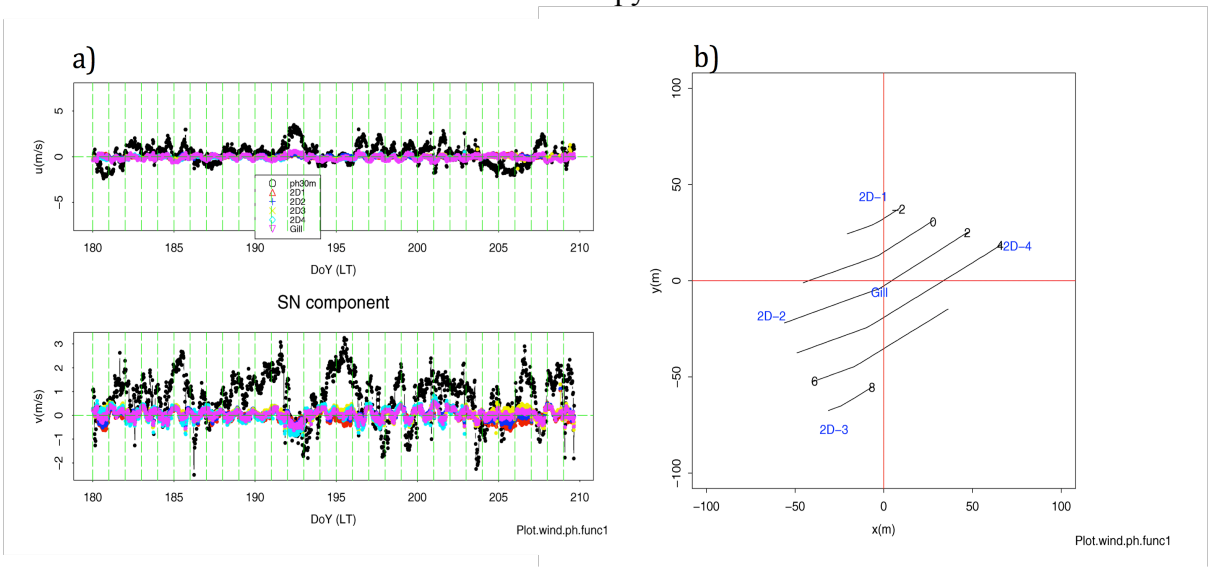

Figure 3: (a) Time series of sonic wind speed components (u, the E-W component, and v, the N-S component) for the Spring/Summer 2008 campaign. Ph30m is Campell Sci. CSAT sonic anemometer at the flux tower, 2D1, 2D2, 2D3, 2D4, and Gill are the ATI 2D and Gill 3D sonic anemometers in the subcanopy layer. (b) Horizontal locations

of the subcanopy array and tower setup. The origin is at the tower flux location. Black lines and numbers correspond to the local topography contours (m).

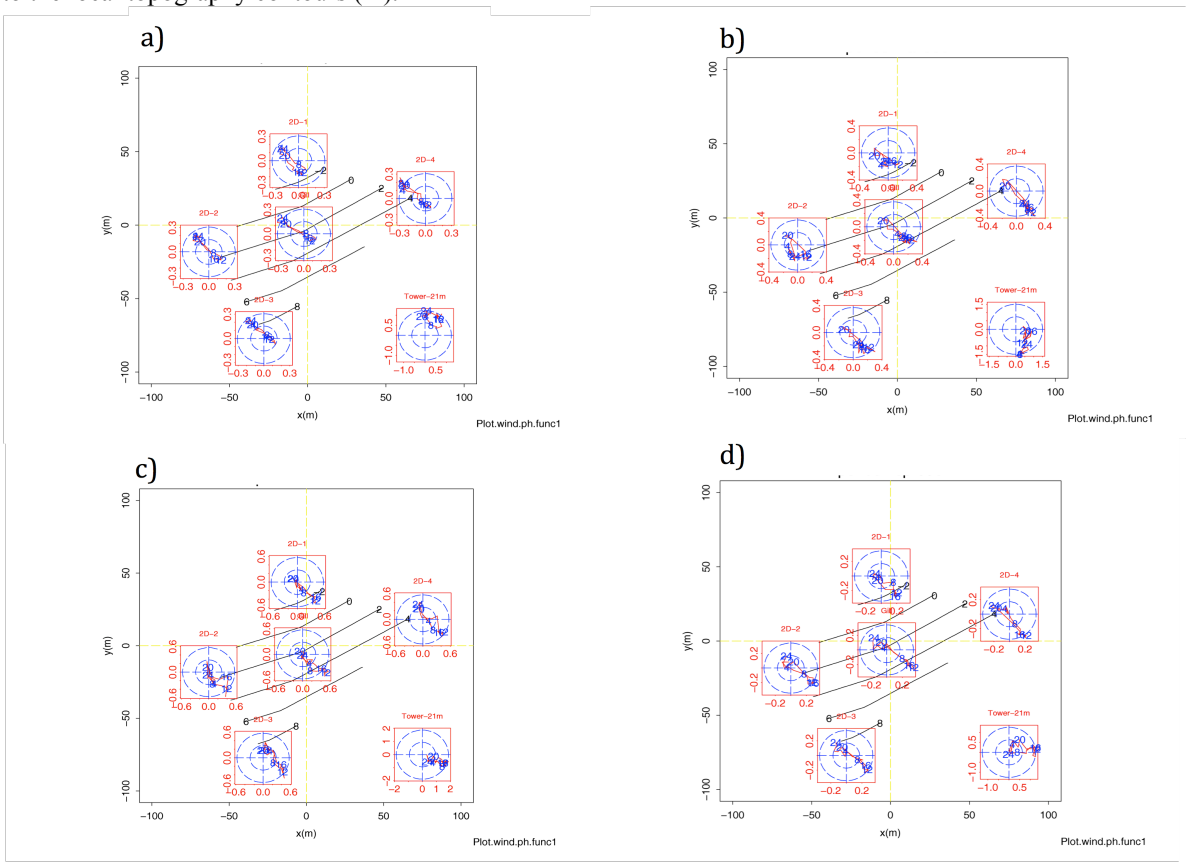

Figure 4: Hourly hodographs for spring/summer 08 (a), Fall 08 (b), winter 08/09 (c), and spring 09 (d) for the subcanopy and at the top of the tower (on the bottom right side) sonic anemometers. Numbers in the hodographs are the local time hour. Black lines are the local elevation contours relative to the tower elevation.

Marked spatial differences on CO_2 concentrations are only observed with leaf coverage. During late fall, winter, and at the beginning of spring the CO_2 concentration field is nearly homogeneous near the forest floor. Fig. 5 shows CO_2 concentration and its deviation from the subcanopy spatial mean for summer 2008 and spring 2009. When the canopy starts to leaf out; CO_2 deviations become significant (Fig. 5 b and d). The biggest spatial differences are found during summer, principally at nighttime (Fig. 5a and c). Higher locations (#3 and #4) present the lowest concentration, principally during nighttime. This emphasizes that the drainage flow can deplete some CO_2 to lower grounds at night. One interesting observation is that during some period the higher locations (#3 and #4) had a higher CO_2 concentration than the lower locations (#1, #2), the most noticeable occurred during DOY 204-206 2008 (Fig. 5a). This occurs when there winds are easterly at canopy top (Fig. 3a). Previous studies [*Hadley and Kuzeja*, 2004; *Hadley et al.*, 2008] showed that anomalous high nighttime CO_2 fluxes were observed with easterly wind.

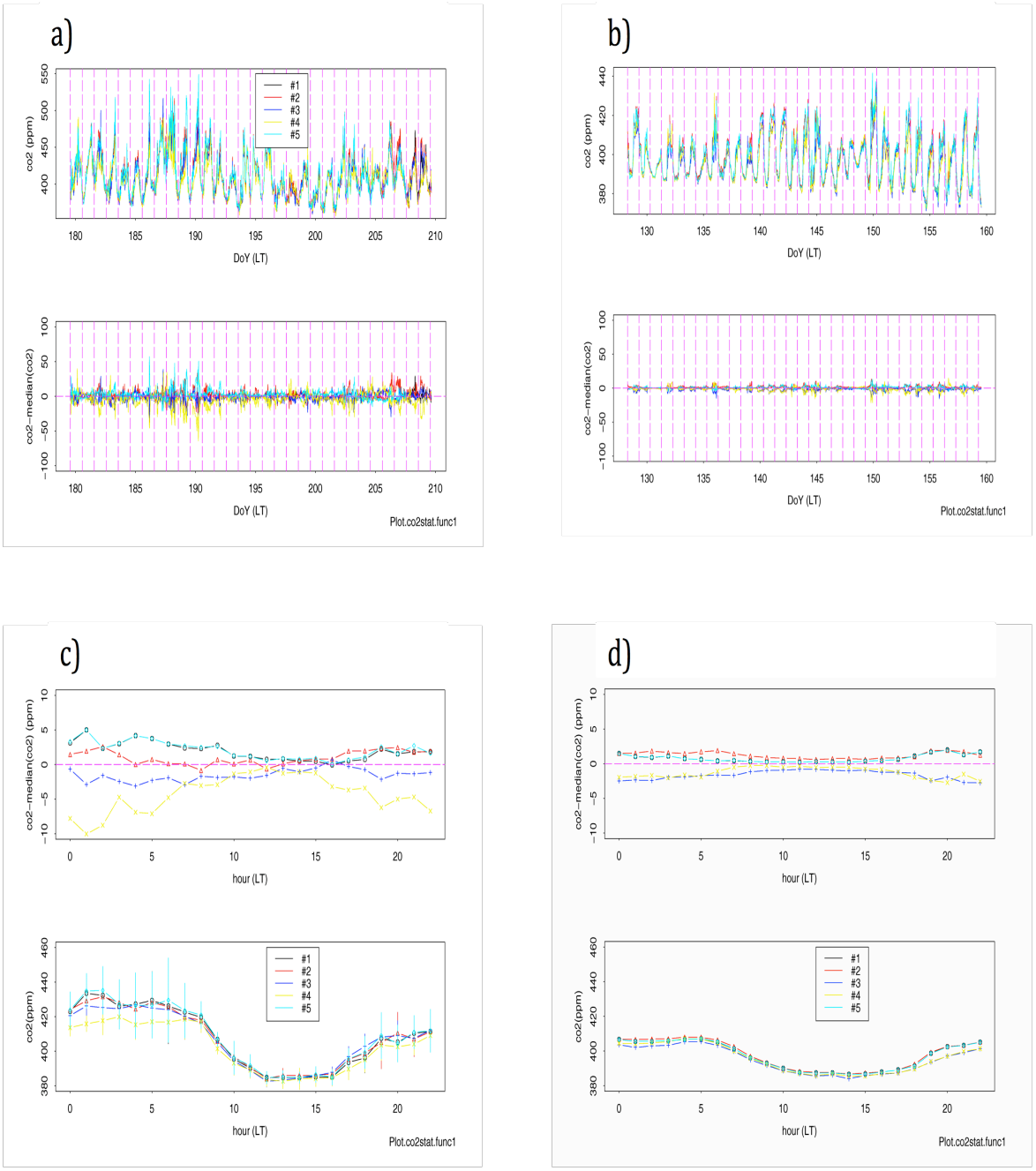

Figure 5: Time series of CO_2 concentration and perturbation at the subcanopy surface array for summer 2008 (a) and spring 2009); (b). Locations #1, #2, #3, #4, and #5 are related to 2D1, 2D2, 2D3, 2D4, and, Gill respectively. (c) and (d) correspond to the mean hourly values of the CO_2 concentration and CO_2 concentration deviations for summer 2008, and spring 2009 respectively.

b. CO_2 Budget – integrating Subcanopy array data w/ Tower flux data.

Turbulent fluxes were calculated using the deviations of a 30-minute centered running mean. Spectral analyses of the flux product wCO_2 at tower top (21 m) indicates that this filter allows low frequency oscillations to be detected. Moreover, the same analysis shows that there is only

small high frequency loss of wCO_2 due to the tube attenuation. The observed median diurnal variation of wCO_2 above the vegetated surface (Fig 6ab) shows the expected strongest CO_2 uptake during the day in summer. Nocturnal values of wCO2 are similar in summer and spring. Nocturnal values of the friction velocity (u_*) are larger in spring than in summer, indicating that a leafless canopy produces more wind shear (Figs. 6ab). In the day, seasonal differences are not large. The accumulation of CO_2 within the atmospheric canopy layer determined by calculating the vertical averaged CO_2 tendency from the tower data. Figures 6c, d illustrate the distinct diurnal CO_2 accumulation pattern. Data from the subcanopy array data allow us to calculate the horizontal advection ($advCO_2$), in which we assumed that the CO_2 and wind profiles at the boundaries of the domain are the same as at the tower location. Figures 6cd show that only during spring is there significant daytime CO_2 entry into the domain. There is clear nocturnal CO_2 loss due to a persistent downslope drainage flow (Fig. 4).

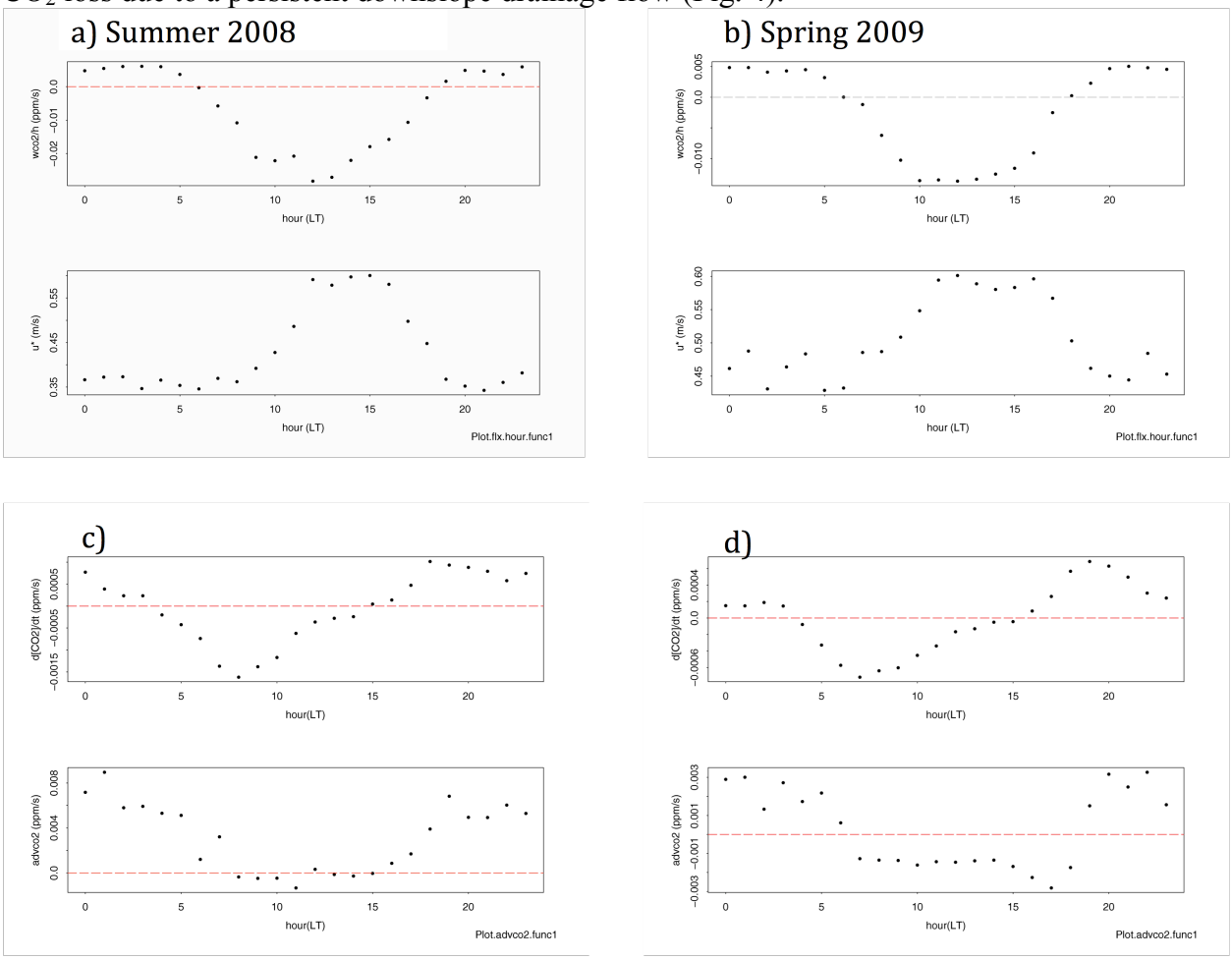

Figure 6: Median hourly values. Top a) and b) flux for summer 2008 and spring 2009. Bottom: a) and b) friction velocity for summer 2008 and spring 2009. Top c) and d)CO_2 accumulation for summer 2008 and spring 2009. Bottom c) and d) Horizontal advection for summer 2008 and spring 2009 using a shape factor of 0.2 [*Staebler and Fitzjarrald*, 2004]. Sign convection: CO_2 leaving the domain => $advCO_2$ >0; CO_2 entering the domain: $advCO_2$ <0.

These observations show that the canopy storage is less important than either the flux through canopy top or the advection on the sides of the domain. (Note that we performed no 'u_* filtering' [*Goulden et al.*, 1996] for the CO_2 flux.) At night, horizontal advection is about the

same magnitude as the observed vertical flux, occasionally exceeding the above-canopy average CO_2 flux.

c. Observations of flow over Prospect Hill, HF

The two sodars are deployed to examine airflow over the HF topography. Data from the top of EMS tower and the lowest level of data from the nearby sodar (nominally 15 m above canopy) show good agreement during the day, when convective mixing homogenizes the wind profile (Fig. 7). At night the tower observations fall below 1 m/s on days 200-203 as expected on a calm night with an overlying stable layer; the two agree on subsequent windy nights.

The case in Fig. 7 is instructive since synoptic weather changes presented us with a period of westerly winds followed by days with easterly winds. We were surprised to discover that the sodar mean vertical wind values agreed fairly well with those seen by the sonic anemometer at the tower (Fig. 7, lowest panel), bearing in mind the expected noise in this signal. We see that $w < 0$ when the EMS tower is on the lee side of Prospect Hill (W wind) and $w > 0$ when the EMS tower was on the windward side (E wind).

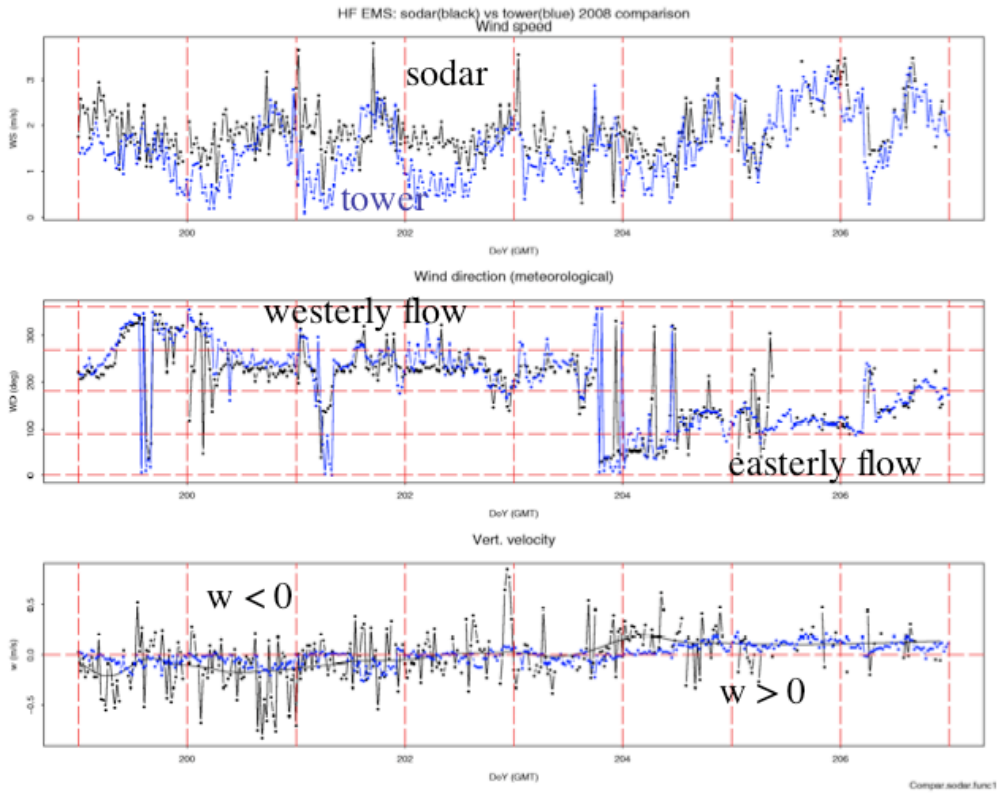

Fig. 7. Winds at the PA0 sodar (black) lowest reporting level and the EMS tower (blue) at the EMS site days 199-207, 2008. Top: wind speed (m/s); middle: wind direction (degrees) ; bottom: vertical velocity (m/s). Solid lines are smoothed versions of the half-hourly data.

We analyzed sodar data from the Soil Warming Site (the PA1 shown in Fig. 2). This site is not ideal for these measurements. Its choice reflects a balance between adequate housing for our computer and minimal annoyance for the resident scientists and staff at Harvard Forest. In preliminary analysis, however, we have found that data from this site can be suitably filtered to provide useful information. We discontinued sodar measurements at this site after we suffered considerable damage by vandals, effectively destroying our sodar.

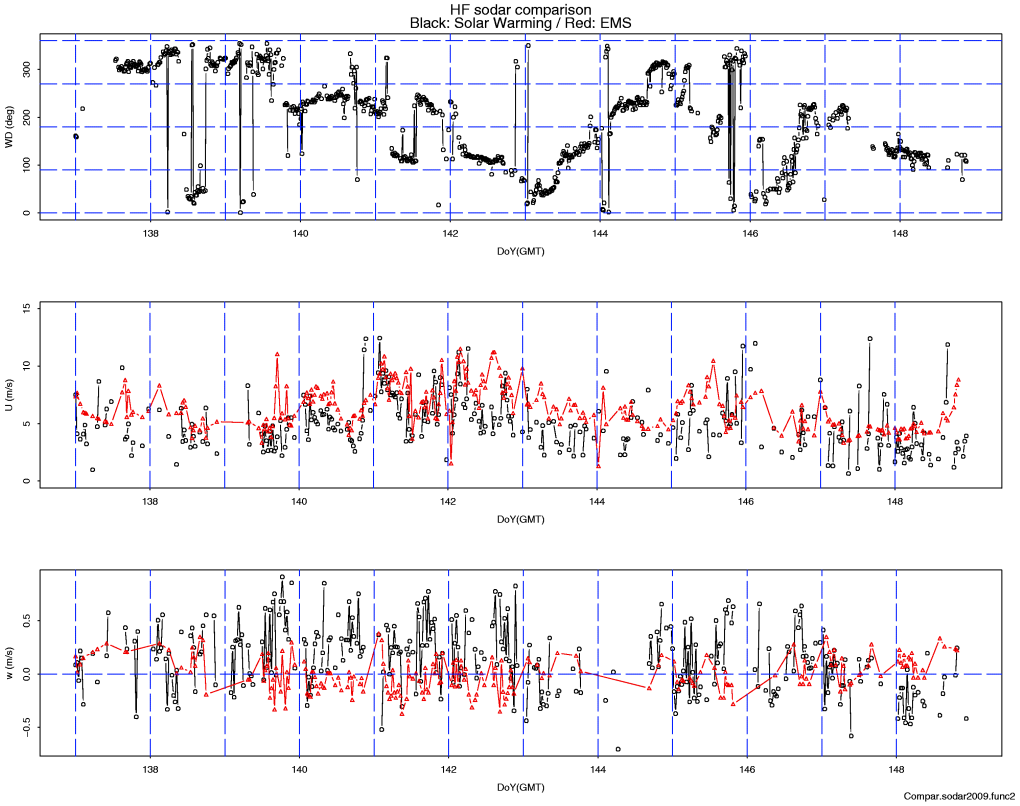

Fig. 8. 2009 DOY 137-48 (UT) half-hourly time series comparison of (top) wind direction; (middle) wind speed and (bottom) mean vertical wind speed between the EMS site PA0 sodar (red, triangles) and the soil warming site PA1 sodar (black, squares).

We use sodar echo strength to estimate the nocturnal boundary layer thickness. Our previous work indicated that *at night*, the 'INVI' parameter from the REMTECH PA0 (a 'proprietary' calculation) was a good indicator of the shear zone delineating the top of the stable boundary layer [*Garstang et al.*, 2005]. In the current deployment, preliminary analysis (e.g. Fig. 9) confirms this idea. We see that the stable boundary thickness, perhaps most appropriate to a mesoscale region around the EMS tower, is 150-200 m thick.

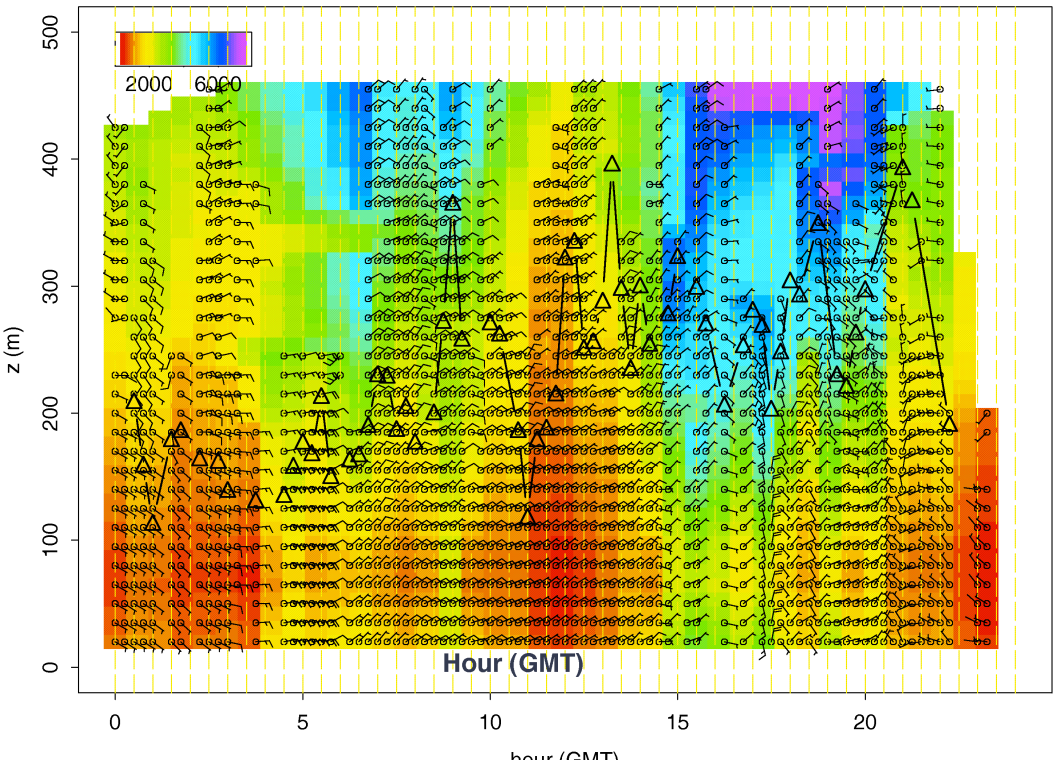

Figure 9. April 16, 2009 (DOY 106) example of EMS site PA0 sodar echo strength (color code, arbitrary units). Time series of the INVI parameter (triangles) tracks the thickness of the stable boundary layer.

4. Continuing data analysis and publication plans.

Subcanopy flow characteristics

During the final phase of this project, we will use the profiles of CO_2 during summer 2009 we make with the in-canopy tethered balloon system to test the 'shape factor' similarity hypothesis that we introduced previously [*Staebler and Fitzjarrald*, 2004] and currently used by others [e.g., *Leuning et al.*, 2008]

An important issue in assessing the role of scalar advection of the mean flow in subcanopy levels is to determine the mean flow angle. What constitutes horizontal or vertical advection given topographical slope? *Finnigan* [2004] argued that tilt corrections to the sonic anemometer vertical velocity are essential if one is to estimate vertical advection for CO_2 budgets in and above forests. *Leuning et al.* [2008] examined three weeks' data and claimed that sonic-based vertical advection cannot be ignored when assessing subcanopy scalar budgets near a gully in Australia. However, *Vickers and Mahrt* [2006] concluded that "…estimates of advection of carbon dioxide based on mass continuity are more plausible than estimates based on the tilt correction methods," much the same conclusion as that of *Staebler and Fitzjarrald* [2004] With the information given by the Gill sonic tilt meter, topographic, and sodar data we will be able to determine the differences from the flow angle to the topographic slopes. We believe that with such information we can investigate the streamline flow in the subcanopy and above the canopy level to partition correctly the horizontal and vertical advection.

Radiation components: making calibration/intercomparisons

This essential topic has no clear 'home' in the current project but it must be done to maintain the value of the long time series of radiative fluxes at the HF EMS site. During the final year of this project we will bring transfer standard instruments for a long (1-3 months) intercomparison period for the radiative flux components (short- and long-wave and PAR; upwelling and downwelling). We have continued these measurements to the present, using funds from a follow-on DOE grant and also resources from ASRC.

Sodar observations at the Hemlock tower, Harvard Forest.

These measurements were accomplished thanks to additional funds we received to participate in a wind energy siting survey. It is included here because the observations also fit perfectly into the ambitions we had in the DOE-supported work.

The sodar deployment made for the wind energy survey aimed to get measurements as near to the top of Prospect Hill or its neighboring ridges (HF towers and topography are shown in Figure 2). We expected that there would be a situation of 'overspeeding' there, a kind of Bernoulli effect as air is forced into a thinner layer by ambient stability as the hill is approached.

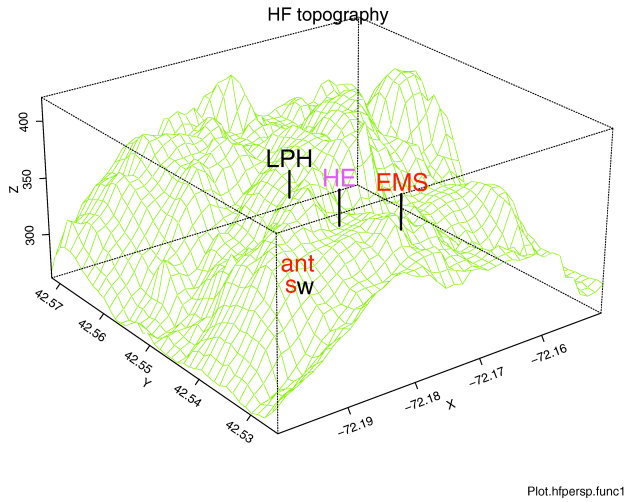

Figure 10. Topography and location of Harvard Forest towers. Measurements made by the ASRC group earlier were at the 'ant' and EMS sites. The current deployment was at the Hemlock tower (HE).

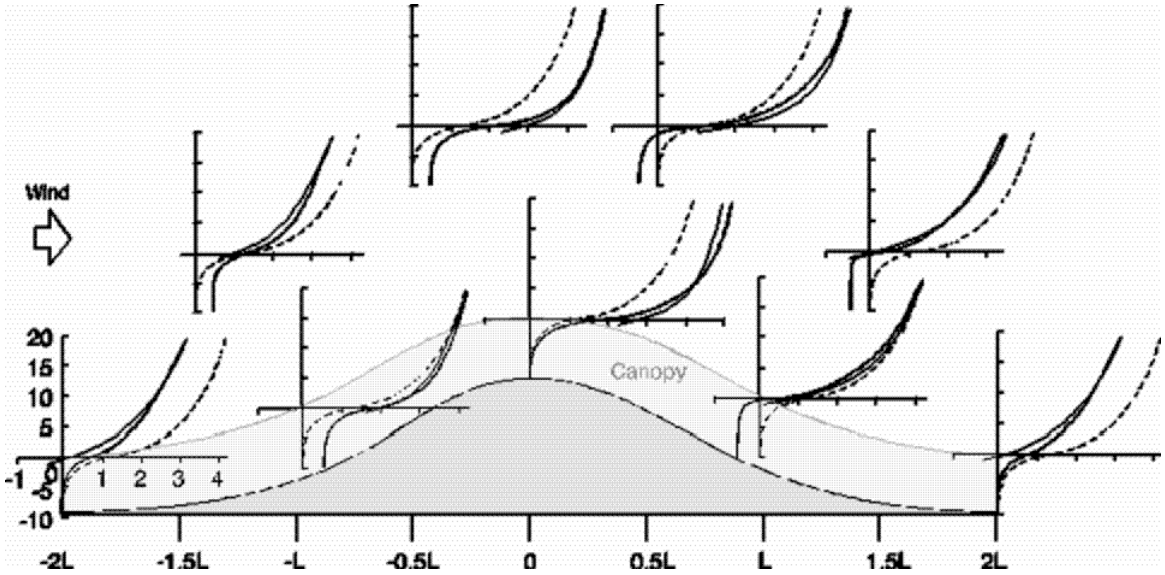

Figure 11. Schematic of the speed-up of flow over a hill with a canopy. (Finnigan and Belcher 2004). Dashed line shows the wind profile well upwind of the hill.

5. Deployment of the sodar at the Harvard Forest Hemlock tower, 2011.

On March 28, 2011, R. Sakai and D. Fitzjarrald, with the help of Mark Van Scoy of HF, installed the PA-0 sodar on the Hemlock tower. We were dismayed to observe that the tower did not stand above the tallest branches. More discouraging was the presence of pipes, one necessarily deploying the sonic anemometer and another holding a toy surveillance camera used to determine whether or not the deciduous trees were in leaf. These obstacles became a large problem for our final ability to obtain more continuous data.

The first data files were obtained on March 28, 2011. From that time until the end of June we were alarmed by the poor data return being obtained. We worked in vain to contact the manufacturer, seeking help to repair our PA-0 sodar.

With the help of HF personnel, we were able to communicate with the sodar remotely from Albany and receive a daily status record during most of the deployment.

Eagerly awaited Remtech engineer M. Rémy Tasso finally came to SUNY at the end of July, whereupon he declared that there was nothing Remtech could do to help us to repair our PA-0 sodar, unless we purchased a $19,000 upgrade. Consequently, we had to replace the PA-0 sodar with the bulkier PA-1 unit. Continuing concerns about the obstacles at tower top led us to put this unit on a raised platform and to rotate the unit by 45° toward the east to give a better clearance for the sodar beams. Data acquisition in this configuration began on July 7, 2011.

The PA-1 sodar survived the difficulties that shut down data acquisition at other HF tower sites in early July, but several days' data were lost owing to power outages. As time went on, there were more periods of missing data, caused by abnormal rainfall (Hurricane Irene and Tropical Storm Lee led to widespread precipitation and sodar data outages even when the power was intact.)

On July 7, we began sodar data acquisition with only 10 levels of wind measurement, at 10-minute intervals. Data were obtained at tower top (canopy level) and at 30-210 m above the canopy, at 20 m intervals. Data collection in this configuration continued until December 13, 2011. Thus, though we were not able to deliver a continuous data set for the 3 months and 2 weeks requested, we operated instruments in the field for 8 months, with nearly 5 months of data

with the instrument in its final configuration. *Please note that the correct way to understand the levels of wind measurement made in this deployment, is measure of the height above the point in the canopy where momentum is absorbed (the 'displacement height' h) NOT the height above the ground.* In this kind of forest, one can usually take the displacement height to be about 75% of canopy height. At this site, this is about 0.75*30 ≈ 22 m. So a measurement at the sonic anemometer at tower top would be nominally at 8 m altitude. The other sodar measurement levels would typically be the output altitude + 8 m.

To complement the sodar data, we obtained data from the sonic anemometer at the top of the Hemlock tower. These data, originally taken at a 5 Hz data rate, were averaged into 10-minute blocks, with the nominal time being the end time of the period. This made the anemometer data averaging in line with the sodar output. Data processed included wind components, as well as the momentum, heat, water vapor and CO_2 eddy fluxes.

Figure 12. View of the Hemlock tower during the deployment. Photos of the deployment are available at: ftp://boojum.asrc.cestm.albany.edu/pub/HF_WIND_ENERGY/HF_sodar_2011_photos/ .

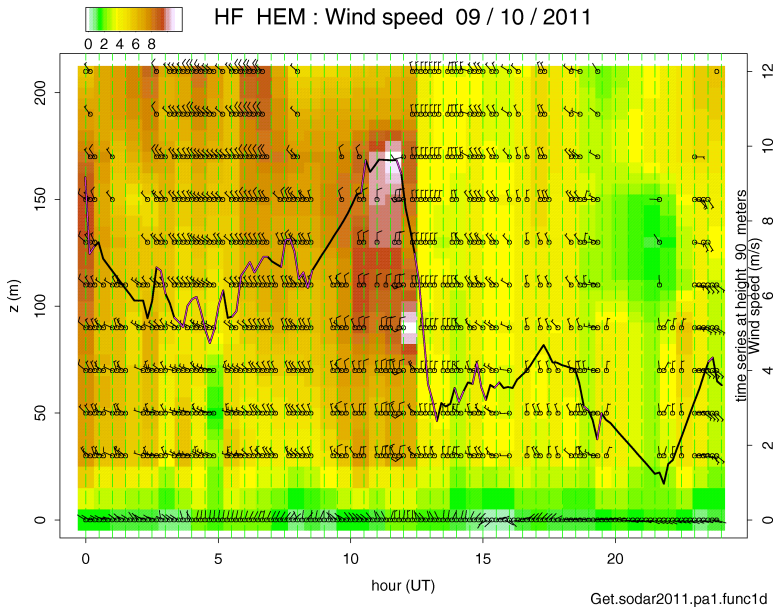

Figure 13. A time-height section for September 10, 2011. Data at the lowest level is the sonic anemometer. Plots such as this are available for all operational days at:
ftp://boojum.asrc.cestm.albany.edu/pub/HF_WIND_ENERGY/HF_sodar_2011_plots/

Assessment of the final data set.

The REMTECH data in the manufacturer's ASCII for the July-November period are available at: ftp://boojum.asrc.cestm.albany.edu/pub/HF_WIND_ENERGY/SODARrawFILES/ . At the same web site, a linear data file "**HEM.HF.SODallLG.README**" (column information) and "**HEM.HF.SODallLG.dat**" (ASCII data, space-delineated) suitable for incorporation into Excel that merges the tower sonic anemometer data with the data from the sodar is available at: ftp://boojum.asrc.cestm.albany.edu/pub/HF_WIND_ENERGY/ .

The sodar obtains its signal from scattering from anomalies the atmospheric density field, which is largely influenced by temperature and, to a degree by humidity fluctuations. These are typically the result of turbulence. During periods of extreme calm there are fewer echoes with which to obtain the wind measurement. As a remote sensing device, the sodar can only obtain an estimate of the winds when a sufficient number of echo returns are available. The sonic anemometer at tower top, in contrast, is almost an *in situ* device, since it measures wind speed by time-of-travel differences over a distance of only a few centimeters. The REMTECH sodar does not allow the user to alter the data quality criteria. The manufacturer has assured me in person that he does not want to see unreliable data being used, but he is sufficiently concerned about proprietary rights that details of this process are not publicly available. Given this issue, exacerbated by the difficulties of blockage of the sodar location at tower top, our data return was not what would be expected from an open flat site away from the forest. When we can find

$19,000, we hope to upgrade our newest sodar to improve performance. Overall, there was a data recovery rate of about 40%.

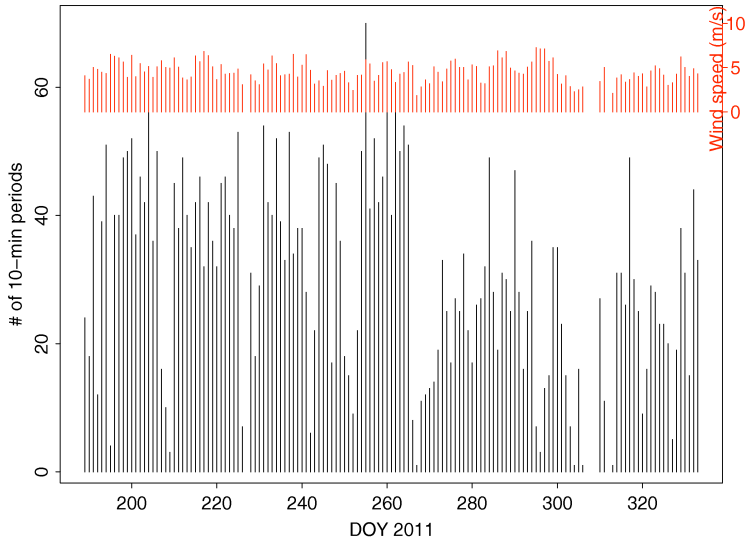

Figure 13. Daily rate of data recovery % though the course of the deployment for the 50 m level. In red are the daily-averaged sodar wind speed at the 50 m level.

The flatness of the wind profile is likely due to two factors: a) the 'tower' wind speed is highly sheltered, with treetops, video cameras and all manner of obstacles obstructing the flow and b). Since the Hemlock tower is near the top of a ridge, and one expects 'overspeeding' there (cf. Figure 3). This diminishes its value compared to what might occur at a flat site, well above the canopy. That we could use the sonic anemometer data from tower top illustrates the role of coupling to the rough surface has on the difference in wind speed aloft and near the canopy. Thus, we see that the hour of maximum median winds at the tower top is during the day. Aloft, the maximum winds are at night, during stable conditions, when the forest is largely decoupled from the boundary layer above.

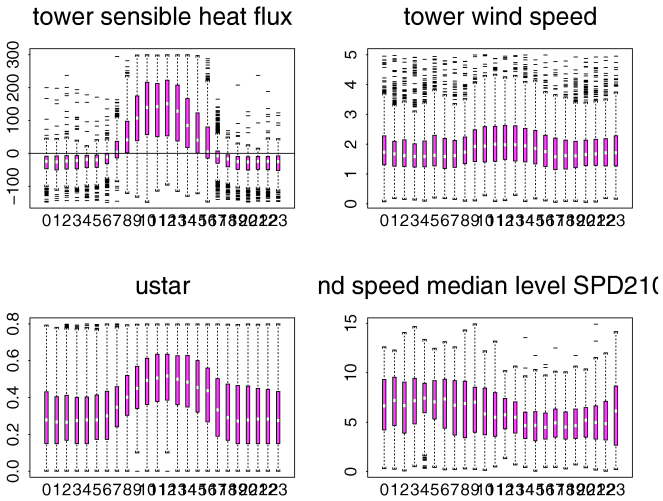

Figure 14. 'Box plots' for the 24-hour cycle, with medians, quartiles and outliers for the sensible heat flux, tower wind speed, ustar (a measure of momentum coupling or friction between the wind and the canopy) the median wind ,

and the median wind speed at the 210 m sodar level.

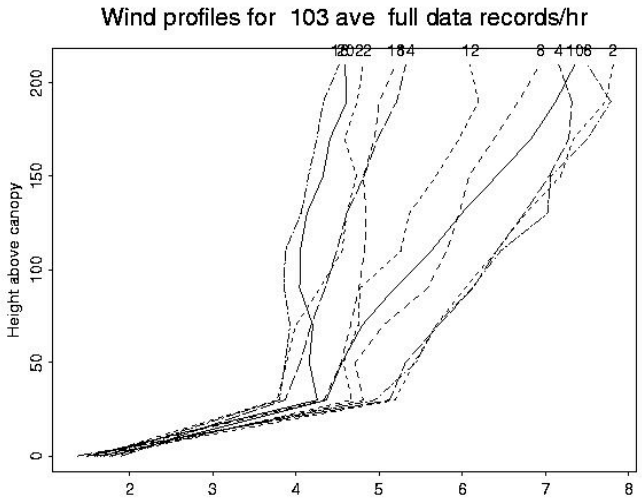

*Figure 15. Selection of data using only 10-minute periods for which **all** levels from the tower up to 210 m were reporting valid winds. One can see how the median wind profile shifts through the day and the coupling between forest and wind aloft occurs during the day and the increase in nocturnal wind. Numbers at the top of the plots at the hours plotted. (Odd hours omitted in the plot for clarity.) Selections: 2479, number of 10-minute periods with all 11 wind levels reporting; 7044, number of periods with at least 6 wind levels reporting.*

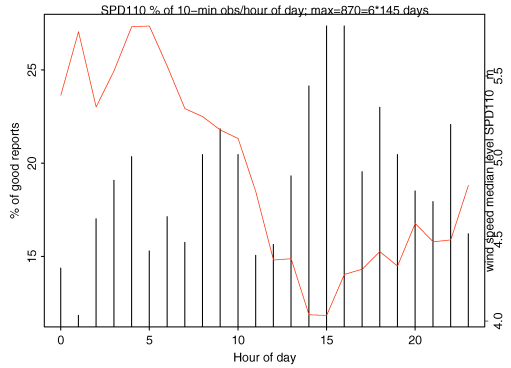

Figure 16. Percentage of data available by hour of day for the 110 m sodar level, along with the median wind speed by hour (red).

6. Presentations and publications.

We made poster presentations at the Harvard Forest Ecology Symposium, 2009, 2010 and submitted an abstract in 2011. We made two presentations at the 29th AMS Conference on Agric. and Forest Meteorology, 2010. Two papers are in draft form and will be submitted during 2013.

P1.26 Advective and topographic influences on eddy flux measurement
David R. Fitzjarrald, University at Albany / SUNY, Albany, NY; and R. Sakai, J. Hadley, and J. W. Munger

Using arguments are based on scale analyses, wind tunnel experiments, and large eddy simulations, several authors have argued that Bernoulli effects associated with flow over hills strongly affect subcanopy motions, possibly altering horizontal CO_2 advection. We report on our efforts to detect these effects at a well-studied site with complicated topography.

Observations have been made over a period of three years aimed to describe how boundary layer flow over topography at Harvard Forest MA influences subcanopy flows. We have continued to operate the subcanopy array at the Little Prospect Hill (LPH) tract. In one season, we installed two sodars, one upwind and one downwind of the prominent topography. We characterize above-canopy flows by direction and intensity, comparing the flow upwind and downwind of the major topographic features. Separately, we show a well-defined anabatic-katabatic subcanopy flow pattern. We examine the extent to which subcanopy flows may or may not be altered by the flow aloft, estimating a relevant Froude number to facilitate comparison with earlier work. During the growing seasons, we operated a subcanopy CO2 array to assess horizontal advective effects. The final step is to document any effects that may modify horizontal advection on the subcanopy CO2 budget.

2:45 PM5.6 **Forest response to cloud and canopy effects on incident radiation**

David R. Fitzjarrald, University at Albany / SUNY, Albany, NY

In the 17 years since I first met Andy Black, eddy flux observations have gone from being an exotic rarity to a commodified ‘gap-filled' data product, a trade perhaps like replacing venison for processed canned meat product. There are, of course, real needs to have easily accessed homogeneous data sets with which to assess model outcomes. However, does this mean that the field micrometeorologist is readily (or ready to be) supplanted by technicians?

Correctly describing the light environment impinging upon the forest canopy and penetrating to the forest floor still remains a challenge. Moreover, few efforts have been made to date to examine the consequences that evolving and thriving in a fluctuating light environment has on canopy carbon dioxide (Fco2), heat (H) and water vapor (LE) fluxes. (See Doughty et al., 2006). The eddy covariance method as conventionally performed is not suitable to address this issue. In this presentation, I will report what kinds of transient light regimes are produced by clouds and canopy. In addition, I will discuss briefly how one may develop data analysis approaches that invoke alternate ways to interpret the ensemble mean at the heart of the EC method, following earlier work by Czikowsky and Fitzjarrald (2009). This is an event-based compositing approach to estimate H, LE and Fco2.

To describe the radiation environment of the upper and lower canopy, during the field phases of LBA-ECO our team operated the laser ceilometer at the km67 site near Santarém Pará Brazil and an array of 16 subcanopy radiation sensors. One sensor was a PAR sensor; the remaining were pyranometers, multiplexed every 10 seconds. In conjunction with G. G. Parker (Smithsonian Environmental Research Center, MD), measurements of the spectral character of subcanopy light were made during July 2004, to account for spectral response differences between the global solar and PAR sensors. Recording these data on the same time base as the above-canopy radiation and fast-response flux sensors, facilitate comparison of the influence of clouds on radiation at both levels.

References

Czikowsky, M. J., and D. R. Fitzjarrald (2009), Detecting rainfall interception in an Amazonian rain forest with eddy flux measurements, Journal of Hydrology, 377(1-2), 92-105, doi:10.1016/j.jhydrol.2009.08.002.

Doughty, C. E., M. L. Goulden, S. D. Miller, and H. R. da Rocha (2006), Circadian rhythms constrain leaf and canopy gas exchange in an Amazonian forest, Geophys. Res. Lett, 33, L1

7. References.

Acevedo, O. C., R. da Silva, D. R. Fitzjarrald, O. L. L. Moraes, R. K. Sakai, and M. J. Czikowsky (2008), Nocturnal vertical CO2 accumulation in two Amazonian ecosystems, *Journal of Geophysical Research-Biogeosciences*, *113*.

Belcher, S. E., and B. Reading (2008), Onset of drainage currents in flows over forested hills, in *18th Symposium on Boundary Layers and Turbulence*.

Falge, E., D. Baldocchi, R. Olson, P. Anthoni, M. Aubinet, C. Bernhofer, G. Burba, R. Ceulemans, R. Clement, and H. Dolman (2001), Gap filling strategies for defensible annual sums of net ecosystem exchange.,

Finnigan, J. J. (2004), A re-evaluation of long-term flux measurement techniques Part II: coordinate systems, *Boundary-Layer Meteorology*, *113*(1), 1-41.

Finnigan, J. J., and S. E. Belcher (2004), Flow over a hill covered with a plant canopy, *Quarterly Journal of the Royal Meteorological Society*, *130*(596).

Fitzjarrald, D., and K. Moore (1990), Mechanisms of nocturnal exchange between the rain forest and the atmosphere, *Journal of Geophysical Research*, *95*(D10), 16839-16850.

Garstang, M., D. R. Fitzjarrald, K. Fristrup, and C. Brain (2005), The Daily Cycle of Low-Frequency Elephant Calls and Near-Surface Atmospheric Conditions, *Earth Interactions*, *9*(14), 1-21.

Goulden, M. L., J. W. Munger, S. M. Fan, B. C. Daube, and S. C. Wofsy (1996), Measurements of carbon sequestration by long-term eddy covariance: methods and a critical evaluation of accuracy, *Global Change Biology*, *2*(3), 169-182.

Hadley, J. L., and P. S. Kuzeja (2004), Carbon and water exchange of a younger, drier deciduous forest compared to the long-term study site at Harvard Forest, Massachusetts, in *American Geophysical Union, Spring Meeting 2004, abstract# B13A-04*.

Hadley, J. L., P. S. Kuzeja, M. J. Daley, N. G. Phillips, T. Mulcahy, and S. Singh (2008), Water use and carbon exchange of red oak-and eastern hemlock-dominated forests in the northeastern USA: implications for ecosystem-level effects of hemlock woolly adelgid, *Tree Physiology*, *28*(4), 615.

Karipot, A., M. Y. Leclerc, G. Zhang, T. Martin, G. Starr, D. Hollinger, J. H. McCaughey, and G. R. Hendrey (2006), Nocturnal CO 2 exchange over a tall forest canopy associated with intermittent low-level jet activity, *Theoretical and Applied Climatology*, *85*(3), 243-248.

Katul, G. G., J. J. Finnigan, D. Poggi, R. Leuning, and S. E. Belcher (2006), The influence of hilly terrain on canopy-atmosphere carbon dioxide exchange, *Boundary-Layer Meteorology*, *118*(1), 189-216.

Leclerc, M. Y., A. Karipot, T. Prabha, G. Allwine, B. Lamb, and H. L. Gholz (2003), Impact of non-local advection on flux footprints over a tall forest canopy: a tracer flux experiment, *Agricultural and Forest Meteorology*, *115*(1-2), 19-30.

Lee, X. (2000), Air motion within and above forest vegetation in non-ideal conditions, *Forest Ecology and Management*, *135*(1-3), 3-18.

Lee, X. (1997), Gravity waves in a forest: a linear analysis, *Journal of the Atmospheric Sciences*, *54*(21), 2574-2585.

Lee, X., H. H. Neumann, G. Hartog, R. E. Mickle, J. D. Fuentes, T. A. Black, P. C. Yang, and P. D. Blanken (1997), Observation of gravity waves in a boreal forest, *Boundary-Layer Meteorology*, *84*(3), 383-398.

Leuning, R., S. J. Zegelin, K. Jones, H. Keith, and D. Hughes (2008), Measurement of horizontal and vertical advection of CO2 within a forest canopy, *Agricultural and Forest Meteorology*, *148*(11), 1777-1797.

Mahrt, L. (2008), The Influence of Transient Flow Distortion on Turbulence in Stable Weak-Wind Conditions, *Boundary-Layer Meteorology*, *127*(1), 1-16.

Mahrt, L., D. Vickers, R. Nakamura, M. R. Soler, J. Sun, S. Burns, and D. Lenschow (2001), Shallow Drainage Flows, *Boundary-Layer Meteorology*, *101*(2), 243-260.

Nappo, C. J., D. R. Miller, and A. L. Hiscox (2008), Wave-Modified Flux and Plume Dispersion in the Stable Boundary Layer, *Boundary-Layer Meteorology*, *129*(2), 211-223.

Percival, D. B., and A. T. Walden (2000), *Wavelet methods for time series analysis*, Cambridge University Press.

Poggi, D., and G. Katul (2007), The ejection-sweep cycle over bare and forested gentle hills: a laboratory experiment, *Boundary-Layer Meteorology*, *122*(3), 493-515.

Ross, A. N. (2008), Large-eddy simulations of flow over forested ridges, *Boundary-Layer Meteorology*, *128*(1), 59-76.

Staebler, R. M., and D. R. Fitzjarrald (2005), Measuring canopy structure and the kinematics of subcanopy flows in two forests, *Journal of Applied Meteorology*, *44*(8), 1161-1179.

Staebler, R. M., and D. R. Fitzjarrald (2004), Observing subcanopy CO2 advection, *Agricultural and Forest Meteorology*, *122*(3-4), 139-156.

Sun, J., S. P. Burns, A. C. Delany, S. P. Oncley, A. A. Turnipseed, B. B. Stephens, D. H. Lenschow, M. A. LeMone, R. K. Monson, and D. E. Anderson (2007), CO2 transport over complex terrain, *Agricultural and Forest Meteorology*, *145*(1-2), 1-21.

Sun, J., R. Desjardins, L. Mahrt, and I. MacPherson (1998), Transport of carbon dioxide, water vapor, and ozone by turbulence and local circulations, *Journal of Geophysical Research-Atmospheres*, *103*(D20).

Thomas, C., and T. Foken (2007), Organised motion in a tall spruce canopy: temporal scales, structure spacing and terrain effects, *Boundary-Layer Meteorology*, *122*(1), 123-147.

Vickers, D., and L. Mahrt (2006), Contrasting mean vertical motion from tilt correction methods and mass continuity, *Agricultural and Forest Meteorology*, *138*(1-4), 93-103.